Systems & Control Transactions

Research Article - Peer Reviewed Conference Proceeding
ESCAPE 35 - European Symposium on Computer Aided Process Engineering
Ghent, Belgium. 6-9 July 2025
Jan F.M. Van Impe, Grégoire Léonard, Satyajeet S. Bhonsale,
Monika E. Polańska, Filip Logist (Eds.)

PSE PRESS

A Comprehensive study on PHB biosynthesis and biodegradation through kinetic modelling

Ariyan Amirifar[a], Constantinos Theodoropoulos[a,*]

[a] Department of Chemical Engineering, Biochemical and Bioprocess Engineering Group, The University of Manchester, Manchester M13 9PL, UK
* Corresponding Author: k.theodoropoulos@manchester.ac.uk

ABSTRACT

Polyhydroxyalkanoates (PHAs) are microbial bioplastics that are fully biodegradable, biocompatible and can be produced by renewable feedstocks through fermentation. These are all desirable attributes for the replacement of current fossil-based plastics. Strong mathematical models describing bioprocesses are invaluable tools that can be used for enhancing bioprocess understanding as well as optimization. In this study, polyhydroxybutyrate (PHB), by *Cupriavidus necator* DSM 545 was produced using glycerol and ammonium sulphate (AS) as the sole carbon and nitrogen sources, respectively. In addition, a kinetic bioprocess model was developed. The kinetic parameters of the model were calibrated with five fermentation experiments with different initial conditions (e.g. variable glycerol and AS concentrations) in order to properly establish the inhibition regions and provide a generalized model as much as possible. The model was successfully validated by three independent experiments, two with extreme and one with moderate initial conditions. In addition, the analysis of the data provided valuable metabolic insights for this bioprocess. It was shown that the PHB storage capacity of cells strongly correlates with the initial nitrogen concentration in the medium, meaning that efforts for maximizing biomass production in a two-stage bioprocess strategy should be carefully designed so that the nitrogen concentration does not irreversibly compromise the maximum PHB accumulation potential. Furthermore, a preliminary kinetic analysis of the biodegradation of solvent casted PHB films was performed.

Keywords: Fermentation, Genetic Algorithm, Modelling, Modelling and Simulations, PHB, *C. necator* DSM 545

1. INTRODUCTION

Some 80% of all plastics globally produced have accumulated in or leaked to the environment [1]. Over 99.5% of plastics are currently being derived from petroleum-based resources [2]. A promising alternative to conventional fossil-based plastics is polyhydroxyalkanoates (PHA), microbial bioplastics synthesized through fermentation of renewable feedstocks, with poly(3-hydroxybutyrate) (PHB) being the most extensively studied variant [2]. The primary contributors to the high cost of PHA production are feedstock costs, which account for up to 50% of total production costs [3], alongside low PHA yields [4]. Crude glycerol, the primary byproduct of biodiesel production, representing about 10% w/w of the produced biodiesel, could be further valorised to PHB as the fermentation's main carbon source [5]. *Cupriavidus necator* DSM 545, is a well-studied microorganism able to consume glycerol as sole carbon substrate for the production of PHB[6–9], with productivities as high as 1.4 g/L/h[8]. *C. necator* DSM 545 along with *Zobellella denitrificans* MW1 are the only two reported microorganisms able to produce PHB on glycerol with productivities higher than 1 g/L/h[10]. Mathematical models are invaluable tools for the optimization and design of bioprocess and few studies have attempted to describe and/or optimize the production of PHB on glycerol by *C. necator* DSM 545 using such models[6–8,11].

In this work, a detailed macroscopic kinetic model was developed based on experimental observations to describe the batch fermentation of *Cupriavidus necator* DSM 545 under controlled pH (6.8) and DO (30% of saturation) conditions on a chemically defined mineral medium with glycerol and ammonium sulphate (AS) as the

carbon and nitrogen sources, respectively. The model was tuned on experimental data from batch fermentations. Sensitivity analysis was also performed. Batch was the preferred mode of operation to identify inhibition regions with respect to carbon and nitrogen sources, and to gain insight into the behavior and metabolic state of the microorganism for fermentations conducted with different initial conditions. Finally, the model was validated using experiments with initial conditions that were not used in the parameter tuning process.

2. MATERIALS AND METHODS

2.1 Microorganism and culture conditions

Cupriavidus necator DSM 545 was used as the microorganism for all fermentations. The master stock has been extensively adapted to glycerol previously in our research group and stored in cryovials at -80°C during their mid-exponential phase [7]. The fermentation medium was adapted from Kim et al[12]. The cultivation process has been described elsewhere [6,7]. Bioreactor fermentations were carried out in 0.5 L or 3 L Applikon bioreactors (Getinge, NE) under the following controlled conditions: 30°C, pH 6.8, dissolved oxygen at 30% saturation (achieved by automatic control of agitation speed and air flow rate, max 2vvm), and 10% mid-exponential phase inoculum. The pH of the medium was adjusted automatically using a 2M KOH solution. For fermentation follow up, 5 mL samples were taken in duplicate from each bioreactor at different time points for further analysis. All procedures were carried out aseptically where appropriate.

2.2 Biodegradation experiments

Compost was sourced from the Firs botanical grounds (University of Manchester, UK) as the biological environment to isolate an efficient PHB degrading microorganism. This 6-month-old compost was produced from garden waste and local kitchen food waste and sieved on-site (mesh size < 10 mm). A small amount of compost sample was spread on mineral PHB agar plate incubated at 37 °C for 48 h [13]. The microorganisms capable of growing on the plates were further isolated on the same plate recipe until a single colony type was achieved. The colonies were identified via sequencing of the 16S or 18S/28S RNA gene (for bacteria or fungi, respectively). Amplification was performed via colony PCR using GoTaqGreen® master mix (Promega, UK). Thereafter, the amplified gene was separated via gel electrophoresis and the Monarch® DNA gel extraction kit (New England Biolabs®, UK). The NCBI BLAST tool (NCBI) was used on the obtained sequence to annotate the taxonomy of the microorganisms. The PHB obtained from one of the fermentation experiments (biodegradation substrate) was casted on a petri dish using chloroform or hexafluoroisopropanol (HFIP) as solvent in $\frac{1g\ PHB}{25\ mL\ solvent}$ ratio. The isolated microorganism was thereafter inoculated (10% w/w) in 5 mL of appropriate medium and culture conditions, together with PHB films, in glass test tubes.

2.3 Analytical procedures

Cell dry weight (CDW) was measured gravimetrically as described previously[7]. The absorbance of each sample was measured at 600 nm using a UV spectrophotometer (UV-1280, Shimadzu®) to monitor microbial growth, particularly during the initial hours of fermentation. A correlation between cell dry weight (CDW) and optical density (OD) was established (R^2=0.9687) to account for potential inaccuracies in CDW measurements. PHB was quantified via Gas chromatography coupled with a Flame Ionization Detector (GC-FID, Agilent) using the method optimized by Lanham et al.[14]. Analysis was performed in an HP-5 column (Agilent J&W GC columns) with helium as the carrier gas and a split ratio of 1:10. Oven temperature was initially set to 80°C for 5 minutes, then ramped up to 280°C at 20°C/min, with a 2-minute hold. Calibration was performed using commercial methylated 3-HB (Sigma-Aldrich) in chloroform. Glycerol in sample supernatant was monitored via High-Performance Liquid Chromatography (HPLC) [7]. Total nitrogen concentration in sample supernatant was quantified via a total nitrogen analyser (TOC/TN multi N/C 3100, Analytik Jena). For this, 100 µL of the filtered supernatant was injected. After catalytic combustion, nitrogen oxide reacts with ozone to form excited states, emitting light upon returning to the ground state. This light, measured by a chemiluminescence detector, is proportional to the nitrogen content. Ammonium sulphate solutions in distilled water served as calibration standards. Scanning Electron Microscopy (SEM) of the PHB films were acquired by Zeiss Ultra 55 microscope. The samples were sputter coated with 80:20 Ad:Pd. Atomic Force Microscopy (AFM, Bruker) with probes of 4 N/m force constant was used.

2.4 Parameter tuning and sensitivity analysis

The kinetic constants of the model were tuned by minimizing the normalized mean squared error between experimental and predicted data (equation 1).

$$\min G(kk) = \sum_h^{n_h} \sum_j^{n_j} \sum_i^{n_i} \left(\frac{Z_{h,j,i}^{Exp}(kk) - Z_{h,j,i}^{Pred}(kk)}{\max\left(Z_{h,j,i}^{Exp}(kk)\right)} \right)^2 \qquad (1)$$

Here G is the objective function, Z represents experimental and predicted data sets, and kk the parameter set. Indices n_i, n_j, and n_h correspond to the number of independent variables, data points, and training data sets, respectively. The minimization problem was solved using Matlab genetic algorithm (ga) to avoid local minima, followed by the deterministic function fmincon to refine solutions. Thereafter, sensitivity analysis was performed to assess the most sensitive parameters. For this purpose,

a normalized sensitivity parameter was used [15]:

$$S_{y/p} = \frac{dy_i}{dp_i} \cdot \frac{p_{0,i}}{y_{0,i}} \quad (2)$$

Here $\frac{dy_i}{dp_i}$ is the change of the model output y_i in response to a change in a model parameter pi (5% perturbation was chosen) and $y_{0,i}$ is the model output when the parameter $p_{0,i}$ is set to its original value $p_{0,i}$. A positive sensitivity value translates into an increased model response when a parameter increases, whereas negative sensitivity values signify the opposite behaviour[15].

3. RESULTS AND DISCUSSION

3.1 Model development

Five state variables were considered for the model: residual biomass (xR), total nitrogen (N), Glycerol (S_1), PHB (P), and citric acid (S_2) concentrations. These variables were correlated by kinetic equations (equations 3-7) using their corresponding rate terms.

$$\frac{dx}{dt} = r_{xR}x \quad (3)$$

$$\frac{dN}{dt} = (q_{N,S_1} + q_{N,S_2})x \quad (4)$$

$$\frac{dS_1}{dt} = q_{S_1}x \quad (5)$$

$$\frac{dS_2}{dt} = q_{S_2}x \quad (6)$$

$$\frac{dP}{dt} = q_P x \quad (7)$$

3.1.1 Biomass formation

Literature and experimental observations confirm that too high or too low of glycerol or AS negatively affects cell growth [6–9]. It has been reported that 30 g/L glycerol (as sole carbon source) and 2 g/L of AS (as sole nitrogen source) are the thresholds above which significant cell growth inhibition occurs for *C. necator* DSM 545 [16,6,7]. Nonetheless, these studies have evaluated the nitrogen inhibition ranges in shake flask experiments, which might be different than bioreactor fermentations where the pH of the media and oxygen levels are strictly controlled. To establish the nitrogen inhibition region for the model, five fermentations were carried out with 30 g/L of glycerol and varying initial AS concentrations ranging from 0.8-7.4 g/L. Figure 1 shows that the maximum residual biomass (xR) concentrations increase with AS across the entire range, although the increase rate gradually diminishes. Hence, 2 g/L of AS was not the growth inhibition threshold for the bioprocess in bioreactor fermentations. On the other hand, PHB concentration decreases significantly above 3.4 g/L AS. To account for glycerol and nitrogen inhibition effects on growth, Monod kinetics with Haldane inhibition terms[17] were applied on AS and glycerol as the limiting substrates (equation 8). Moreover, it was realized that the initial citric acid (CA) present in the medium formulation was first consumed as the preferred carbon substrate for growth before the cells began to metabolise any glycerol, having a boosting effect and eliminating the growth lag phase normally observed on glycerol. Therefore, the rate of biomass formation should be composed of two segments: biomass production on CA or biomass production on glycerol, starting only after CA depletion. The inhibition of CA on glycerol consumption was modelled via Hill kinetics [18]. Growth on citric acid was inhibited at high nitrogen concentrations (data not shown) hence it was necessary to consider Haldane inhibition kinetics for nitrogen also.

$$r_{xR} = \mu_{S_1} + \mu_{S_2} = \mu_1 \frac{S_1}{\frac{S_1^2}{K_{iS_1}} + S_1 + K_{S_1}} \cdot \frac{N}{\frac{N^2}{K_{iN}} + N + K_N} \cdot \frac{1}{1 + k_{S_2}(S_2)^{n_{S_2}}} + \mu_2 \frac{S_2}{S_2 + K_{S_2}} \frac{N}{\frac{N^2}{K_{iN,S_2}} + N + K_{N,S_2}} \quad (8)$$

Here μ_1 and μ_2 are specific growth rates [h^{-1}]; and K_{S_1}, K_N and K_{S2}, K_{N,S_2} pairs are the saturation constants for glycerol and CA, respectively [g/L]; K_{iS_1}, K_{iN} and K_{iN,S_2} are the inhibition constants [$(g/L)^2$] for glycerol and CA, respectively; n_{S_2} is a Hill coefficient.

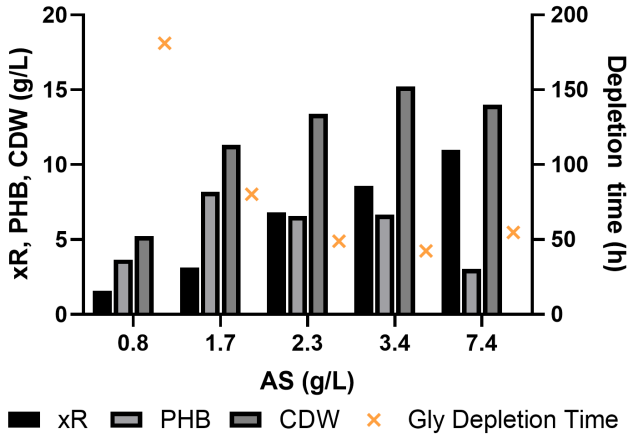

Figure 1. Cell dry weight (CDW), residual biomass (xR), PHB end values and glycerol depletion time vs. different initial AS concentrations (30 g/L glycerol).

Another interesting observation is that the glycerol depletion time heavily relied on the initial AS concentrations, e.g. ~2.3-3.4 g/L of AS resulted in lower depletion time and higher biomass growth, but was detrimental to the PHB concentrations.

3.1.2 PHB production

The maximum PHB titer profile against initial AS concentrations in Figure 1 matches expectations, as it is well-known that the presence of nitrogen inhibits PHB production, and that PHB production favours high C/N ratios unlike biomass growth where lower C/N values are preferred[6,7]. PHB accumulation is predominantly induced by nitrogen limitation[7]. However, PHB synthase is a constitutive enzyme in *C. necator* [19], justifying partially growth-associated PHB production [9,20]. Hence, the

Luedeking-Piret model[21] was chosen to describe PHB production (equations 9-11). Throughout the nitrogen limited phase, it is expected that the carbon source should be mostly directed towards PHB production[22,23]. It has been reported however, that PHB production could halt prior to carbon source depletion[22]. This could be due to the fact that the size and number of PHB granules are theoretically capped by a regulatory system involving phasin proteins[22,24], or due to the fact that prolonged nitrogen starvation impairs the activity of PHB synthase. In order to account for such an effect, some studies have introduced powered inhibition functions in the PHB production rate equation[8,22]. However, it was realized in this study that no matter how much of the initial carbon source was allocated to biomass production, no more PHB was produced up to a certain extent even if glycerol was present after reaching the biomass stationary phase. According to Figure 2 the maximum PHB accumulation capacity of cells could be correlated to the initial total nitrogen concentration through the Haldane inhibition model (equation 6).

$$q_P = \alpha r_{xR} + \beta \times \left(1 - \left(\frac{f}{f_{max}}\right)^m\right) \quad (9)$$

$$\beta = \frac{\mu_P S_1}{S_1 + K_{S,P} + S_1^2/K_{iS,P}} \cdot \frac{1}{1 + k_{N,P} + N^{n_P}} \quad (10)$$

$$f_{max} = \frac{c(N_0 - h)}{\frac{(N_0 - h)^2}{d} + (N_0 - \mathrm{h}) + e} \quad (11)$$

α is the growth-associated constant for PHB, and β the non-growth associated parameter; $f\ (\frac{PHB}{CDW})$ and f_{max} are the PHB accumulation extent term, and its maximum, respectively; N_0 is the initial total nitrogen concentration in the broth [g/L]; c, d, and e are constants (c=3.3854 h^{-1}, d=0.2302 g/L, e=0.2771 g/L, h=0.1323 g/L).

3.1.3 Substrate and nutrient uptake

CA, glycerol and nitrogen uptake rates were necessary to compute new kinetic constants for the nitrogen uptake rate with nitrogen self-inhibition effect on growth utilising Haldane inhibition kinetics (equation 15).

$$q_{S_2} = \frac{1}{Y_{\frac{xR}{S_2}}} \mu_{S_2} \quad (12)$$

$$q_{S_1} = \frac{1}{Y_{\frac{xR}{S_1}}} \mu_{S_1} \quad (13)$$

$$q_{N,S_2} = \frac{1}{Y_{\frac{xR}{N}}} \mu_{S_2} \quad (14)$$

$$q_{N,S_1} = \frac{\mu_N S_1}{S_1 + K_{N,S_1}} \cdot \frac{N}{\frac{N^2}{K_{iN,N}} + N + K_{N,N}} \quad (15)$$

Y_{xR/S_2}, Y_{xR/S_1} and $Y_{\mathrm{xR/N}}$ are CA, glycerol and nitrogen to biomass yields, respectively. μ_N is the specific nitrogen consumption rate (h^{-1}), K_{N,S_1}, $K_{N,N}$ and $K_{iS,N}$ are saturation and inhibition constants (g/L), respectively.

3.1.4 Model performance

Based on a 5% perturbation of the 36 kinetic constants, a range of average sensitivity values from 2.5×10^{-8} to 12.5 was produced. It was decided to consider a sensitivity value threshold of ≥0.1, resulting in 13 sensitive parameters (final values in Table 1). The calibration data (figure 3, I-V) cover glycerol and nitrogen concentrations 13-43 g/L and 0.29-1.56 g/L, respectively. The independent validation data (figure 3, i-iv) was able to predict the state variables dynamics at extreme initial glycerol and nitrogen concentrations, 55 g/L and 2.53 g/L respectively, among milder conditions within the region of the values of the calibration data.

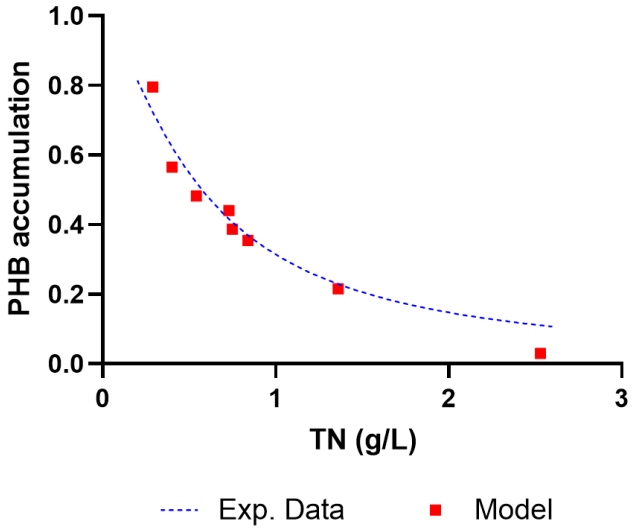

Figure 2. Emperical relationship between maximum PHB accumulation and initial nitrogen concnentration in the medium (R^2=0.9347).

Table 1: Values of the most sensitive model parameters.

Parameter	Value	Unit
$k_{N,P}$	141	g/L
$Y_{\frac{xR}{N}}$	3.15	g/g
μ_2	0.9079	h^{-1}
$K_{iS,P}$	25.8064	g/L
K_N	0.3851	g/L
$Y_{\frac{xR}{S_2}}$	0.8792	g/g
n_P	1.49	-
K_{S_2}	0.2872	g/L
k_{S_2}	74.30	g/L
m	7.98	-
$K_{N,N}$	2.2483	g/L
$Y_{\frac{xR}{S_1}}$	0.3876	g/g
μ_P	0.8437	h^{-1}

3.2 Biodegradation experiments

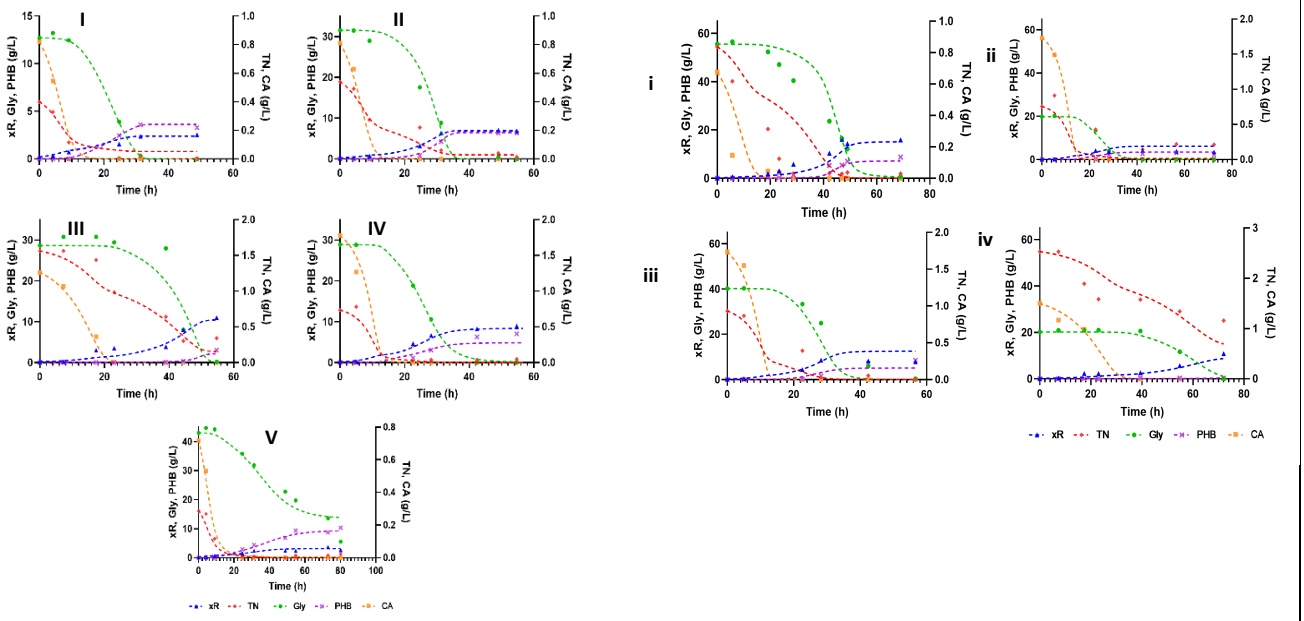

Figure 3: Kinetic model calibration (I-V) and validation (i-iv) runs. Dotted lines represent model predictions; data points are from fermentation experimetns. The state variables are: residual biomass (xR), total nitrogen (TN), glycerol (Gly), PHB and citric acid (CA).

A fungus able to grow on PHB mineral agar plate at 37℃ was successfully isolated from compost, its 28S RNA gene was amplified and sequenced. Based on NCBI BLAST, *Aspergillus fumigatus* produced significant alignment with the sequence, with a 99.11% identity score. The optimal culture conditions were extracted from the the literature[25]; The isolated fungi was cultured in liquid Busshnell-Haas medium (BHM) supplemented with 0.1% w/w PHB, at 45℃, and pH 7 for the biodegradation experiments to be ready for accelerated biodegradation of PHB films. It was desired to assess the biodegradation kinetics of PHB films with different casting solvents. The average initial inoculum was 26 ± 9 ($\times 10^4 \frac{spores}{ml}$). It can be seen from Figure 4 that the casting solvent altered the biodegradation kinetics of the films. The biodegradation behaviour could be modelled through first order kinetics ($-r_{PHB} = km_{PHB}$) giving rise to kinetic constants of 0.3453 and 0.3363 h^{-1} for $CHCl_3$ and HFIP casted films, respectively. HFIP films had a lag phase of ~1 day unlike the $CHCl_3$ casted films. This could be explained through the different morphologies that the solvents produce affecting biodegradation kinetics as it is well-known that the biodegradation of PHB commences through microbial surface erosion. HFIP produced a film with much less surface features and fewer pore sizes but with pores orders of magnitude larger than the $CHCl_3$ casted films (Figure 5). Based on the AFM images, the spherulites of the HFIP casted films were very smooth, separated with rather deep depletion zones, whereas the $CHCl_3$ casted films exhibit many inhomogeneous surface features in the entire imaged area.

CONCLUSIONS

The proposed generalized and improved kinetic model for the production of PHB by *C. necator* DSM 545 on glycerol and AS as carbon and nitrogen sources, respectively, provides valuable metabolic insights regarding PHB accumulation capacity of this microorganism. Moreover, it was found that biodegradation kinetics of solvent-casted PHB films depend on the type of solvent probably because it directly affected film morphology.

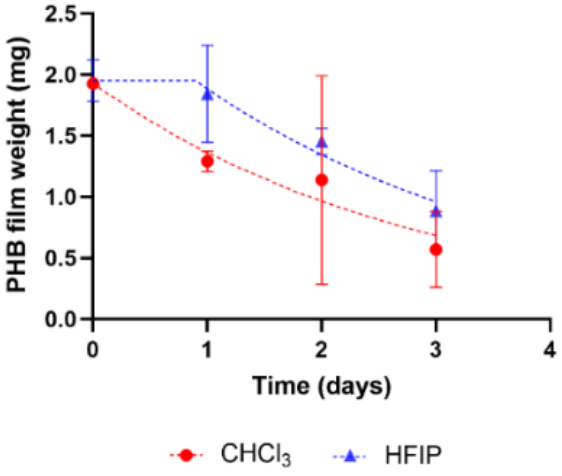

Figure 4. Mass loss of PHB films casted with $CHCl_3$ or HFIP. Dotted lines: first order kinetic model.

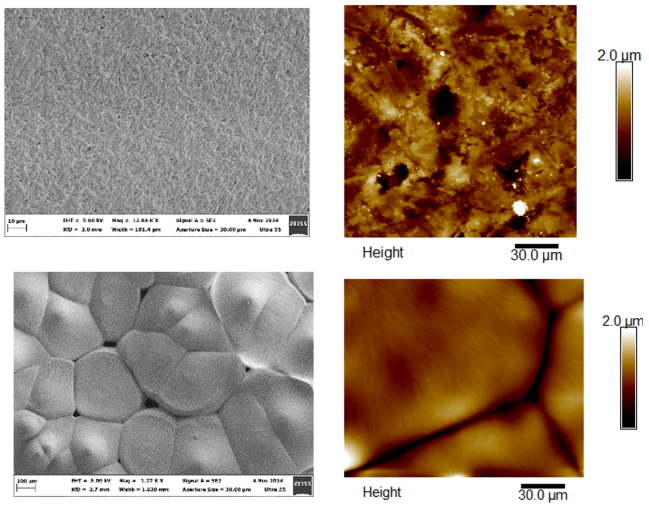

Figure 5. SEM and AFM images for PHB casted with $CHCl_3$ (top) and HFIP (bottom).

ACKNOWLEDGEMENTS

The authors wish to thank the University of Manchester for the provision of a Dean's Doctoral Scholarship Award to Ariyan Amirifar.

REFERENCES

1. Dimante-Deimantovica I, Saarni S, Barone M, et al. Downward migrating microplastics in lake sediments are a tricky indicator for the onset of the Anthropocene. Sci Adv. 2024;10(8):eadi8136.
2. Diankristanti PA, Lin YC, Yi YC, Ng IS. Polyhydroxyalkanoates bioproduction from bench to industry: Thirty years of development towards sustainability. Bioresour Technol. 2024 Feb;393:130149.
3. Park H, He H, Yan X, Liu X, Scrutton NS, Chen GQ. PHA is not just a bioplastic! Biotechnol Adv. 2024;71:108320.
4. Koller M, Mukherjee A. A New Wave of Industrialization of PHA Biopolyesters. Bioengin. 2022 ;9(2).
5. Vlaeminck E, Uitterhaegen E, Quataert K, Delmulle T, De Winter K, Soetaert WK. Industrial side streams as sustainable substrates for microbial production of poly(3-hydroxybutyrate) (PHB). World J Microbiol Biotechnol. 2022 Dec 1;38(12).
6. Sun C, Pérez-Rivero C, Webb C, Theodoropoulos C. Dynamic Metabolic Analysis of Cupriavidus necator DSM545 Producing Poly(3-hydroxybutyric acid) from Glycerol. Processes. 2020;8(6):657.
7. Pérez Rivero C, Sun C, Theodoropoulos C, Webb C. Building a predictive model for PHB production from glycerol. Biochem Eng J. 2016;116:113–21.
8. Mozumder MSI, De Wever H, Volcke EIP, Garcia-Gonzalez L. A robust fed-batch feeding strategy independent of the carbon source for optimal polyhydroxybutyrate production. Process Biochem. 2014;49(3):365–73.
9. Špoljarić IV, Lopar M, Koller M, Muhr A et al. In silico optimization and low-structured kinetic model of poly[(R)-3-hydroxybutyrate synthesis by Cupriavidus necator DSM545 by fed-batch cultivation on glycerol. J Biotechnol. 2013;168(4):625–35.
10. Koller M, Obruča S. Biotechnological production of polyhydroxyalkanoates from glycerol: A review. Biocatal Agric Biotechnol. 2022 Jul;42:102333.
11. Lopar M, Špoljarić IV, Cepanec N, Koller M, Braunegg G, Horvat P. Study of metabolic network of Cupriavidus necator DSM 545 growing on glycerol by applying elementary flux modes and yield space analysis. J Ind Microbiol Biotechnol. 2014;41(6):913–30.
12. Kim BS, Lee SC, Lee SY, Chang HN, Chang YK, Woo SI. Production of poly(3-hydroxybutyric acid) by fed-batch culture of Alcaligenes eutrophus with glucose concentration control. Biotechnol Bioeng. 1994;43(9):892–8.
13. Ramsay BA, Saracovan I, Ramsay JA, Marchessault RH. A method for the isolation of microorganisms producing extracellular long-side-chain poly (β-hydroxyalkanoate) depolymerase. J Environ Polym Degrad. 1994 Jan;2(1):1–7.
14. Lanham AB, Ricardo AR, Albuquerque MGE, Pardelha F, Carvalheira M et al. Determination of theextraction kinetics for the quantification of polyhydroxyalkanoate monomers in mixed microbial systems. Process Biochem. 2013 48(11):1626–34.
15. Zacharopoulos I, Theodoropoulos C. Continuous production of succinic acid from glycerol: A complete experimental and computational study. Bioresour Technol. 2023 Oct;386:129518.
16. Sharmaa K, Srivastava AK, Sreekrishnan TR. Model-based Optimization of Biopolymer Production from Glycerol. Chem Biochem Eng Q. 2021; 35(1):65–80.
17. Haldane JBS. Enzymes. First M.I.T. Press paperback edition. Cambridge, Massachusetts: M.I.T. Press; 1965. 235 p. (M.I.T. paperback series).
18. Kwon YJ, Engler CR. Kinetic models for growth and product formation on multiple substrates. Biotechnol Bioprocess Eng. 2005 Dec;10(6):587–92.
19. Doi Y. Microbial synthesis, physical properties, and biodegradability of polyhydroxyalkanoates. Macromol Symp. 1995 Jul;98(1):585–99.
20. Horvat P, Vrana Špoljarić I, Lopar M, Atlić A, Koller M, Braunegg G. Mathematical modelling and

process optimization of a continuous 5-stage bioreactor cascade for production of poly[-(R)-3-hydroxybutyrate] by Cupriavidus necator. Bioprocess Biosyst Eng. 2013 Sep;36(9):1235–50.
21. Luedeking R, Piret EL. A kinetic study of the lactic acid fermentation. Batch process at controlled pH. J Biochem Microbiol Tech. Eng. 1959 (4):393–412.
22. Tamis J, Marang L, Jiang Y et al.. Modeling PHA-producing microbial enrichment cultures-towards a generalized model with predictive power. New Biotechnol. 2014; 31(4):324–34.
23. Segura PC, Wattiez R, Vande Wouwer A, Leroy B, Dewasme L. Dynamic modeling of Rhodospirillum rubrum PHA production triggered by redox stress during VFA photoheterotrophic assimilations. J Biotechnol. 2022 Dec 10;360:45–54.
24. Mitra R, Xu T, Chen G, Xiang H, Han J. An updated overview on the regulatory circuits of polyhydroxyalkanoates synthesis. Microb Biotechnol. 2022 May;15(5):1446–70.
25. Bhatt R, Patel KC, Trivedi U. Purification and Properties of Extracellular Poly(3-hydroxybutyrate) Depolymerase Produced by Aspergillus fumigatus 202. J Polym Environ. 2010 Jun;18(2):141–7.